

Agglomerative Clustering of Simulation Output Distributions Using Regularized Wasserstein Distance

Mohammadmahdi Ghasemloo¹ and David J. Eckman¹

¹Department of Industrial and Systems Engineering, Texas A&M University, College Station, TX 77843, United States.

mohammad_ghasemloo@tamu.edu, eckman@tamu.edu

Abstract

We investigate the use of clustering methods on data produced by a stochastic simulator, with applications in anomaly detection, pre-optimization, and online monitoring. We introduce an agglomerative clustering algorithm that clusters multivariate empirical distributions using the regularized Wasserstein distance and apply the proposed methodology on a call-center model.

1 Introduction

A simulation model is a computational or mathematical representation of a real-world system designed to study its behavior under various scenarios. Simulation models are used extensively in fields such as engineering, economics, healthcare, and environmental science to predict and analyze the outcomes of different scenarios without the need to experiment in the real world, which can be costly, time-consuming, or impractical. Outputs of a simulation model typically correspond to key performance indicators (KPIs) of interest to the decision maker, e.g., profit, throughput, or service level. For stochastic simulation models, simulating a given scenario generates outputs that vary from replication to replication, thus each scenario has an associated probability distribution describing the stochastic behavior of its outputs. When conducting simulation experiments, the user controls which scenarios are simulated and how many replications are run. Simulation experiments can be easily designed to generate data that satisfies the standard assumptions of being independent and identically distributed, in contrast to most data obtained from the real world. Common tools for analyzing simulation output data include summary statistics (e.g., sample means, variance, and covariances) and visualization tools (e.g., histograms and boxplots). For problems with multiple KPIs, the multivariate empirical distribution produced by the data contains valuable information about system performance, but can be difficult to analyze and plot.

To reveal important patterns and relationships that cannot be detected by conventional data analysis methods, we propose clustering the empirical distributions of simulated scenarios.

Clustering is an unsupervised learning approach that can help discover important patterns and relationships in complex datasets. In the context of simulation output data, clustering can identify scenarios with similar KPIs, or more precisely, similar output distributions. Moreover, clustering facilitates comparative analysis—by understanding the characteristics of each cluster, a decision maker can draw meaningful comparisons and make informed decisions.

We consider three important applications of clustering for enhancing simulation output analysis: *anomaly detection*, which involves identifying and investigating outliers in simulation outputs; *pre-optimization*, which involves formulating simulation-optimization problems and identifying promising initial solutions; and *online monitoring*, which involves tracking the system state over time and using classification methods to detect potentially undesirable system behavior and trigger appropriate actions or alerts.

We propose an agglomerative clustering method that uses the complete-linkage criterion for forming clusters. We choose agglomerative clustering for its flexibility, as it does not require specifying a predetermined number of clusters, and opt for complete linkage because it maintains compact and well-separated clusters. For the algorithm’s measure of dissimilarity between distributions, we choose the regularized Wasserstein distance. The (unregularized) Wasserstein distance quantifies the distance between two discrete probability distributions by the minimum amount of “work”—defined as the product of the probability mass that needs to be moved and the distance it needs to be transported—required to transform one distribution into the other (Villani, 2009). The Wasserstein distance is chosen over other metrics like Kullback-Leibler divergence or Jensen-Shannon divergence due to its ability to handle distributions with non-overlapping supports, as arises when working with continuous-valued empirical distributions. Another advantage of the Wasserstein distance is the notion of a barycenter, which acts like an average among distributions. This property is particularly useful for post-hoc analysis, when desiring to summarize each cluster with a representative distribution (Peyré & Cuturi, 2019; Arjovsky *et al.*, 2017; Cuturi, 2013). However, computing the Wasserstein distance between two discrete distributions entails solving a linear program (Villani, 2009), which could become computationally intensive when working with large datasets. The regularized Wasserstein distance, also known as the Sinkhorn distance, adds an entropic regularization term that promotes smoother transport plans, is easier to compute, and more stable, making it well suited for data-intensive applications (Cuturi, 2013). Our algorithm determines the optimal number of clusters based on the silhouette index (Shahapure & Nicholas, 2020), a centroid-free metric that evaluates clustering quality in terms of intra-cluster and inter-cluster distances.

Clustering has been used for many purposes in many fields, such as analyzing gene expression in bioinformatics (Eisen *et al.*, 1998), market segmentation in economics (Wedel & Kamakura, 2000), and textures and shapes in image processing (Pappas & Jayant, 1989). Hierarchical clustering techniques, specifically agglomerative clustering, build nested clusterings by iteratively merging the two most similar clusters (Murtagh & Contreras, 2012) and produce a dendrogram that depicts the nested clusterings at different levels (Jain *et al.*, 1999). Adaptations like single, complete, and average linkage offer great flexibility in how agglomerative clustering algorithms merge clusters (Jain, 2010). More recently, clustering has been employed in the study of stochastic simulation models, including for simulation optimization (Li *et al.*, 2024; Zhang & Peng, 2024; Peng *et al.*, 2018) and reducing model-form uncertainty (Abdallah *et al.*, 2020). To the best of our knowledge, we are the first to propose agglomerative clustering of simulation output distributions and investigate important use cases.

The Wasserstein distance is used extensively in machine learning applications, such as in computer vision and pattern recognition to robustly compare visual feature distributions (Rubner *et al.*, 2000). For large-scale problems, variations like the entropy-regularized

Wasserstein distance improve computational efficiency. For example, Benamou *et al.* (2015) employ iterative Bregman projections to efficiently solve regularized transportation problems, thereby improving scalability and accuracy. Our clustering framework uses the algorithm of Benamou *et al.* (2015) to calculate the regularized Wasserstein distance and regularized Wasserstein barycenters. For a more detailed overview of computational techniques for optimal transport and its practical applications, we direct the reader to Peyré & Cuturi (2019).

The Wasserstein distance has previously appeared in k -means clustering, e.g., for clustering market regimes (Horvath *et al.*, 2021) and financial data (Riess *et al.*, 2023). Henderson *et al.* (2015) extend the classical k -means algorithm to the clustering of one-dimensional, continuous-valued empirical distributions. However, their clustering algorithm, EP-MEANS, becomes computationally inefficient as the sample size increases and is difficult to extend to multivariate empirical distributions. Zhuang *et al.* (2022) generalize the distance-based formulation of k -means to the Wasserstein space but identify several shortcomings, including the irregularity and non-robustness of barycenter-based Wasserstein k -means. To address scalability issues when clustering discrete distributions, Ye *et al.* (2017) approximate discrete Wasserstein barycenters for large clusters using a modified Bregman alternating direction method of multipliers (ADMM) approach. Our hierarchical clustering algorithm avoids many of these regularity and scalability issues. Chakraborty *et al.* (2020) introduce a hierarchical clustering algorithm that utilizes optimal transport-based distance measures, though the instances being clustered are not themselves distributions, as in our setting.

The rest of this paper is organized as follows: In Section 2, we elaborate on use cases of clustering simulation output distributions. In Section 3, we introduce the relevant notation and propose our agglomerative clustering algorithm. We present the results of several experiments on a call-center staffing problem in Section 4 and conclude in Section 5.

2 Use Cases

We first discuss the utility and versatility of clustering simulation output distributions through several use cases.

Anomaly Detection In the context of simulation experiments, anomalies can be categorized as artificial or systemic. An artificial anomaly is typically associated with logic or coding errors within the simulation model, whereas a systemic anomaly is related to inherent features of the system. When using hierarchical clustering algorithms, anomalous output distributions can be identified by examining the dendrogram, the distances between clusters, or the cluster sizes (Loureiro *et al.*, 2004). After identifying an anomalous output distribution, one would first scrutinize the simulation code to determine if it is an artificial anomaly. If the anomaly is not artificial, then one might investigate further by, for example, examining the marginal distributions, correlation matrices, and corresponding input variables. Hierarchical clustering algorithms such as ours are expected to be more stable for identifying outliers than non-hierarchical clustering methods whose clusterings strongly depend on the initialization of the clusters.

Pre-Optimization In many practical situations, there are tradeoffs between multiple KPIs, and the decision maker may be unable to articulate a priori what constitutes “good” versus “bad” system performance. By clustering output distributions and obtaining the

barycenters, the decision maker can be presented with a more manageable number of distributions to compare. The decision maker could then conduct a series of A/B comparisons, wherein pairs of barycenters are compared and some are eliminated based on unformalized notions of preferred performance until a small number of clusters (or scenarios) remain. The clustering analysis can also help the decision maker specify which metrics should be modeled as objectives in a subsequent simulation-optimization problem and which should be treated as constraints. Achievable thresholds for the constraints can be set based on the observed performance outcomes of the simulated scenarios. Additionally, by examining the inputs associated with scenarios in a promising cluster, the decision maker can identify promising regions of the input space from which to initiate an optimization search, potentially leading to more rapid progress toward the optimal solution.

Online Monitoring This application concerns how the output of a simulation model is influenced by state variables, namely those that evolve over time and can be observed, but not directly controlled, by the decision maker. We envisage an online monitoring framework in which clustering is performed offline and state variables are later tracked in real time with classification algorithms being utilized to help the decision maker anticipate changes in system performance. This approach involves a preliminary simulation experiment in which the scenarios correspond to different initial states, followed by the clustering of the generated outputs. When monitoring the system’s state online, classification algorithms can be used to predict the cluster to which an observed state’s output distribution may belong. Conversely, if the classification algorithm struggles to assign a state to a single cluster, such as a tie when using k -nearest neighbors, it would suggest that system performance may change soon, potentially prompting intervention.

3 Clustering Simulation Output Distributions

Suppose there are N scenarios under consideration, and for each Scenario i , $i = 1, 2, \dots, N$, we obtain n_i independent simulation replications. Let $\mathbf{y}_{il} \in \mathbb{R}^d$ denote the vector output of the l th simulation replication at Scenario i and let $\mu_i := n_i^{-1} \sum_{l=1}^{n_i} \delta_{y_{il}}$ denote the corresponding empirical distribution, i.e., a discrete probability distribution with support $\mathcal{Y}_i = \{\mathbf{y}_{i1}, \dots, \mathbf{y}_{in_i}\}$, where we ignore any duplicate values in the definition of \mathcal{Y}_i , and $\delta_{y_{il}}$ is the Dirac delta function at y_{il} . Since we are interested in clustering $\{\mu_1, \mu_2, \dots, \mu_N\}$, and there is no specific ordering among distributions, we henceforth drop the subscript i and denote the probability mass vector, support, and cardinality of the support of an empirical distribution μ as \mathbf{p}_μ , \mathcal{Y}_μ , and $M_\mu = |\mathcal{Y}_\mu|$, respectively.

3.1 Wasserstein Distance

Let $\Delta_M := \{\mathbf{p} \in \mathbb{R}_+^M : \sum_{l=1}^M p_l = 1\}$ denote the set of all possible probability mass vectors on a support of size M . For two empirical distributions μ and μ' having probability mass vectors $\mathbf{p}_\mu \in \Delta_{M_\mu}$ and $\mathbf{p}_{\mu'} \in \Delta_{M_{\mu'}}$, respectively, the polytope of couplings is defined as

$$\Pi(\mathbf{p}_\mu, \mathbf{p}_{\mu'}) := \left\{ \boldsymbol{\gamma} \in \mathbb{R}_+^{M_\mu \times M_{\mu'}} : \boldsymbol{\gamma} \mathbf{1}_{M_{\mu'}} = \mathbf{p}_\mu, \boldsymbol{\gamma}^T \mathbf{1}_{M_\mu} = \mathbf{p}_{\mu'} \right\},$$

where $\boldsymbol{\gamma}^T$ indicates the transpose of $\boldsymbol{\gamma}$, and $\mathbf{1}_M$ indicates a length- M vector of all 1s. The polytope $\Pi(\mathbf{p}_\mu, \mathbf{p}_{\mu'})$ represents the set of all possible matrices $\boldsymbol{\gamma}$ that redistribute the prob-

ability mass from \mathbf{p}_μ to $\mathbf{p}_{\mu'}$, where each matrix entry $\gamma_{ll'}$ represents the amount of mass transported from the l th element in \mathcal{Y}_μ to the l' th element in $\mathcal{Y}_{\mu'}$ for $l = 1, 2, \dots, M_\mu$ and $l' = 1, 2, \dots, M_{\mu'}$, where the indexing of the supports is arbitrary. The Wasserstein distance between μ and μ' , denoted by $W(\mu, \mu')$, is defined as the optimal value of the following optimization problem:

$$W(\mu, \mu') := \min_{\gamma \in \Pi(\mathbf{p}_\mu, \mathbf{p}_{\mu'})} \langle \mathbf{D}, \gamma \rangle, \quad (1)$$

where $\mathbf{D} \in \mathbb{R}^{M_\mu \times M_{\mu'}}$ is a cost matrix consisting of the pairwise distances between points in \mathcal{Y}_μ and $\mathcal{Y}_{\mu'}$, and $\langle \cdot, \cdot \rangle$ denotes the summation of the element-wise product of two matrices. The optimal solution to the linear program posed in (1), denoted by γ^* , is often referred to as the transportation plan matrix and represents the optimal allocation of probability mass from the source distribution μ to the target distribution μ' . The time complexity of algorithms for computing γ^* is proportional to the cube of the support size (Altschuler *et al.*, 2017; Cuturi, 2013).

The regularized Wasserstein distance, on the other hand, can be solved in near-linear time (Cuturi, 2013) and is defined as

$$W_\lambda(\mu, \mu') := \min_{\gamma_\lambda \in \Pi(\mathbf{p}_\mu, \mathbf{p}_{\mu'})} \langle \mathbf{D}, \gamma_\lambda \rangle - \lambda E(\gamma_\lambda), \quad (2)$$

where λ is a regularization parameter, and $E(\gamma_\lambda)$ is the entropy of the transportation plan matrix γ_λ , defined as $E(\gamma) := -\sum_{l=1}^{M_\mu} \sum_{l'=1}^{M_{\mu'}} \gamma_{ll'} \log \gamma_{ll'}$, where we set $\gamma_{ll'} \log \gamma_{ll'} = 0$ if $\gamma_{ll'} = 0$. As λ approaches 0, the optimal transportation plan matrix for (2), γ_λ^* , becomes more sparse and approaches γ^* (Benamou *et al.*, 2015). The entropic regularization term incentivizes γ_λ^* to be more diffuse than γ^* , and this induced non-sparsity helps to stabilize the computation of γ_λ^* because (2) is a strongly convex program with a unique solution. An advantage of the regularized Wasserstein distance is that γ_λ^* can be calculated through an efficient iterative procedure involving matrix multiplications, as described in Algorithm 1.

Algorithm 1 Regularized Wasserstein distance (Benamou *et al.*, 2015)

Input: $\mu, \mu', \lambda, \mathbf{D}$

- 1: Construct a matrix $\mathbf{Q} \in \mathbb{R}^{M_\mu \times M_{\mu'}}$ having entries $Q_{ll'} = e^{-\frac{D_{ll'}}{\lambda}}$ for $l = 1, 2, \dots, M_\mu$ and $l' = 1, 2, \dots, M_{\mu'}$.
 - 2: Initialize $\mathbf{v}^{(0)} = \mathbf{1}_{M_{\mu'}}$ and $m = 0$.
 - 3: **while** stopping criteria not met **do**
 - 4: Set $\mathbf{u}^{(m)} = \frac{\mathbf{p}_\mu}{\mathbf{Q}\mathbf{v}^{(m)}}$, $\mathbf{v}^{(m+1)} = \frac{\mathbf{p}_{\mu'}}{\mathbf{Q}^T\mathbf{u}^{(m)}}$, and $\gamma_\lambda^{(m)} = \text{diag}(\mathbf{u}^{(m)})\mathbf{Q}\text{diag}(\mathbf{v}^{(m)})$.
 - 5: $m \leftarrow m + 1$.
 - 6: **end while**
 - 7: **return** $W_\lambda(\mu, \mu') = \langle \mathbf{D}, \gamma_\lambda \rangle$.
-

The stopping criteria in Algorithm 1 helps to control the computational cost and could involve setting a maximum number of iterations or stopping when the percentage change in the regularized Wasserstein distance is less than some threshold. The regularized Wasserstein distance plays a central role in our proposed clustering algorithm.

3.2 An Agglomerative Clustering Algorithm

Agglomerative clustering is a hierarchical clustering method that begins by treating each instance as an individual cluster and successively merges the closest pairs based on a specified distance metric, allowing clusters to form organically from the data. We choose to employ agglomerative clustering for several reasons. Firstly, unlike k -means clustering, in which the number of clusters is predefined, agglomerative clustering excels in situations where the optimal number of clusters is unknown. Secondly, centroid-based methods, such as k -means, are sensitive to outliers due to their reliance on a single central point to represent each cluster. Outliers can significantly skew the centroid’s location and distort the clustering process. In contrast, the complete-linkage approach commonly used in agglomerative clustering considers the maximum distance between any two points in distinct clusters, making the clustering more robust to outliers. Complete-linkage clustering also considers the farthest points within the merged clusters, resulting in tighter and more spherical cluster formations compared to single-linkage clustering, which can generate elongated clusters due to chaining effects. Thirdly, agglomerative clustering, particularly when employing complete linkage, offers a valuable output in the form of a dendrogram, which depicts the merging process and the distances between clusters at each stage of the algorithm and can aid in comprehending the relationships between instances and in determining an appropriate number of clusters. Fourthly, unlike the k -means algorithm in which one must repeatedly recalculate the centroid of each cluster, agglomerative clustering does not entail calculating centroids. In our setting, the Wasserstein barycenter is a natural choice of centroid, but lacks robustness (Santambrogio & Wang, 2016); this idiosyncratic behavior of Wasserstein barycenters renders the centroid-based formulation inadequate for representing inter-cluster instances.

To determine the optimal number of clusters, we use the silhouette index proposed by Shahapure & Nicholas (2020). The silhouette index for a given clustering \mathcal{C} is defined as $S_{\mathcal{C}} = \frac{1}{|\mathcal{C}|} \sum_{C \in \mathcal{C}} \frac{1}{|C|} \sum_{\mu \in C} S_{\mu}$, where $S_{\mu} = (b_{\mu} - a_{\mu}) / \max\{b_{\mu}, a_{\mu}\}$, $a_{\mu} = (|C_{\mu}| - 1)^{-1} \sum_{\mu' \in C_{\mu}, \mu' \neq \mu} W_{\lambda}(\mu, \mu')$ is the average regularized Wasserstein distance between μ and every other distribution in the same cluster, and $b_{\mu} = \min_{C' \in \mathcal{C}, C' \neq C_{\mu}} \left\{ (|C'| - 1)^{-1} \sum_{\mu' \in C'} W_{\lambda}(\mu, \mu') \right\}$ is the minimum average distance between μ and distributions in other clusters. The silhouette index considers both intra-cluster (as in a_{μ}) and inter-cluster (as in b_{μ}) distances, and its values fall within the range of -1 to 1 , with a higher silhouette index indicating a more favorable clustering. For an individual distribution μ , a silhouette index S_{μ} close to 1 signifies that μ is well-positioned within its assigned cluster.

We now present Algorithm 2, an agglomerative algorithm for clustering the multivariate empirical distributions of simulation outputs. In Algorithm 2, \mathcal{D} denotes the distance metric used to calculate the cost matrix between points in the supports. Before applying Algorithm 2, the output data is normalized within each dimension to ensure that no one KPI skews the clustering results.

To further assess the practicality of Algorithm 2, it is essential to consider its computational cost. Step 1 of Algorithm 2 calculates the pairwise distances between all distributions, the cost of which scales quadratically with the number of distributions, N . Calculating the regularized Wasserstein distance between a pair of distributions with the same support size exhibits a quadratic dependence on the size of the support (Altschuler *et al.*, 2017). After obtaining the pairwise distances, the rest of Algorithm 2 has a cubic dependence on the

Algorithm 2 Hierarchical Clustering with Regularized Wasserstein Distance

- Input:** $\{\mu_1, \dots, \mu_N\}$, λ , \mathcal{D}
- 1: Compute the regularized Wasserstein distance between all pairs of empirical distributions.
 - 2: Initialize \mathcal{C} as the clustering where each distribution is in its own cluster.
 - 3: **while** $|\mathcal{C}| > 1$ **do**
 - 4: Identify the two clusters C^* and C'^* that are closest to each other based on the complete-linkage distance calculation rule, i.e., $\operatorname{argmin}_{C, C' \in \mathcal{C}} \max_{\mu \in C, \mu' \in C'} W_\lambda(\mu, \mu')$.
 - 5: Merge clusters C^* and C'^* and update \mathcal{C} .
 - 6: Compute the silhouette index for \mathcal{C} .
 - 7: **end while**
 - 8: Choose the clustering with the largest silhouette index.
-

number of distributions (Karthikeyan *et al.*, 2020). Additionally, calculating the silhouette index for a given clustering scales quadratically with the number of distributions (Mur *et al.*, 2016).

3.3 Wasserstein Barycenter

After clustering the distributions, we turn to the regularized Wasserstein barycenter to summarize the information in each cluster. For a given cluster, the regularized Wasserstein barycenter minimizes the average regularized Wasserstein distance between itself and each of the distributions within the cluster, effectively acting as an “average” of the distributions. To compute the barycenter for a cluster C , denoted generically by $\bar{\mu}$, we employ a method that assumes that all distributions have a common support. To conform with this assumption, we manipulate the probability mass vectors of the distributions in each cluster. Specifically, let $\mathcal{Y}_{\bar{\mu}} := \bigcup_{\mu \in C} \mathcal{Y}_\mu$ be the collective support of all distributions in cluster C and let $M_{\bar{\mu}} := |\mathcal{Y}_{\bar{\mu}}|$. For each $\mu \in C$, \mathbf{p}_μ can be modified by extending it to a length of $M_{\bar{\mu}}$ by assigning probability masses of 0 to values in $\mathcal{Y}_{\bar{\mu}} \setminus \mathcal{Y}_\mu$, resulting in a modified distribution $\tilde{\mu}$ defined on $\mathcal{Y}_{\bar{\mu}}$. The regularized Wasserstein barycenter is a discrete distribution on $\mathcal{Y}_{\bar{\mu}}$ having a probability mass vector

$$\mathbf{p}_{\bar{\mu}} := \operatorname{argmin}_{\mathbf{p} \in \Delta_{M_{\bar{\mu}}}} \frac{1}{|C|} \sum_{\mu \in C} W_\lambda(\tilde{\mu}, \bar{\mu}).$$

Although the Wasserstein barycenter can be derived by minimizing a weighted sum of regularized Wasserstein distances, in this paper we assume that the scenarios are equally important, and hence weighted equally. The optimal probability mass vector $\mathbf{p}_{\bar{\mu}}$ can be computed using another iterative procedure, given in Algorithm 3.

4 Experiments

We demonstrate several use cases of the proposed algorithm through experiments involving a discrete-event simulation model of a call center. The call center operates from 8 am to 4 pm and during this time customers call in according to a stationary Poisson process with a rate of 400 customers per hour. This call center serves two classes of customers—regular and premium—with regular customers comprising 60% of incoming calls. Two sets

Algorithm 3 Wasserstein barycenter computation (Benamou *et al.*, 2015)

- Input:** C , λ , \mathbf{D}
- 1: Construct the matrix $\mathbf{Q} \in \mathbb{R}^{M_{\bar{\mu}} \times M_{\bar{\mu}}}$ having entries $Q_{ll'} = e^{-\frac{D_{ll'}}{\lambda}}$ for $l, l' = 1, 2, \dots, M_{\bar{\mu}}$.
 - 2: Initialize vectors $\mathbf{v}_{\mu}^{(0)} = \mathbf{1}_{M_{\bar{\mu}}}$ for all $\mu \in C$.
 - 3: **while** stopping criteria not met **do**
 - 4: **for** $\mu \in C$ **do**
 - 5: Update $\mathbf{u}_{\mu}^{(m)} = \frac{\mathbf{p}_{\bar{\mu}}^{(m)}}{\mathbf{Q}\mathbf{v}_{\mu}^{(m)}}$ and $\mathbf{v}_{\mu}^{(m+1)} = \frac{\mathbf{p}_{\mu}}{\mathbf{Q}^T \mathbf{u}_{\mu}^{(m)}}$.
 - 6: **end for**
 - 7: Compute the current estimate of the barycenter $\mathbf{p}_{\bar{\mu}}^{(m)} = \prod_{\mu \in C} \left(\mathbf{u}_{\mu}^{(m)} \odot (\mathbf{Q}\mathbf{v}_{\mu}^{(m)}) \right)$, where \prod and \odot denote the element-wise product.
 - 8: **end while**
 - 9: Return $\mathbf{p}_{\bar{\mu}}$.
-

of operators—basic service and premium service—provide initial service to regular and premium customers, respectively. If there are no premium customers in the queue, premium service operators can serve regular customers; however, basic service operators cannot serve premium customers. Additionally, 15% of arriving customers, irrespective of their class, abandon if their initial service does not start within a customer-specific amount of time following a uniform distribution between 0.5 and 3 minutes. After their initial service is completed, 15% of customers, irrespective of their class, require additional service that is provided by a third type of operator: technical. Regular and premium customers are served by the same team of technical operators. Service times from basic service, premium service, and technical operators follow exponential distributions with means of 7, 3, and 10 minutes, respectively. Operator-dependent service rates such as these may arise because premium service operators have more resources, full system access, and extensive experience, and therefore can resolve issues more quickly. When queueing for technical support, premium customers are given priority over regular customers, and customers do not abandon. The call center stops receiving new calls at the end of the workday but continues operating until all customers have been served; this policy imposes overwork on the operators.

4.1 Staffing a Fixed Number of Operators

Suppose the call-center manager needs to train 49 operators for some combination of basic service, premium service, and technical roles and is interested in five KPIs: the mean time in the system for regular (Y_1) and premium customers (Y_2), and the mean overwork time for basic service (Y_3), premium service (Y_4), and technical operators (Y_5). Assuming that there must be at least one operator of each type, there are 1128 possible staffing configurations (scenarios). We show that even when simulating a fraction of these configurations, clustering can provide valuable insights about the system’s behavior. We choose 100 configurations that uniformly cover the space of all configurations and simulate 40 days (replications) under each configuration. We then apply Algorithm 2 to cluster the obtained empirical distributions for the five KPIs. The dendrogram in Figure 1 shows the hierarchical clustering of the simulated configurations. Based on the silhouette index plot shown in Figure 1, having 7 clusters is a good choice, though having 8 or 9 clusters would also be satisfactory.

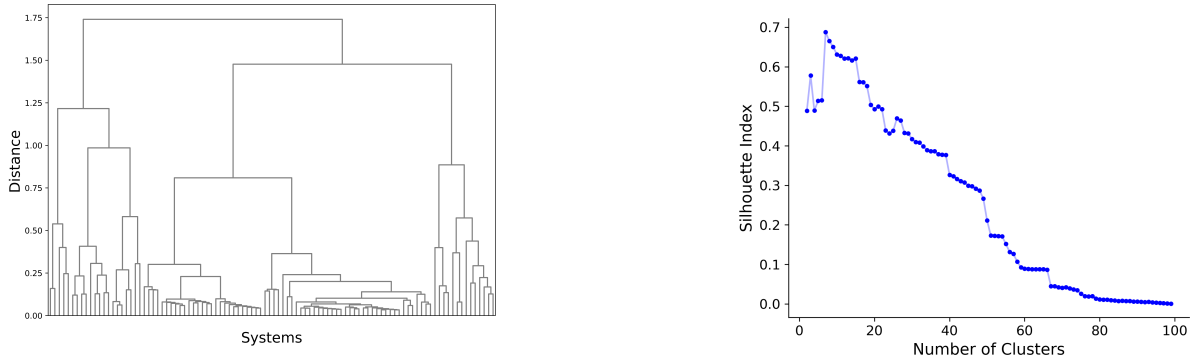


Figure 1: (Left) Dendrogram from clustering the output distributions of 100 staffing configurations. (Right) Silhouette index for different clusterings produced by Algorithm 2.

To more deeply understand the distributions within each cluster, we compute the barycenters of each cluster and plot the marginal cumulative distribution functions (cdfs) for each of the five KPIs. In Figure 2, we observe that no cluster consistently outperforms the others, however, Cluster 4 performs well across all five KPIs, whereas the other clusters perform poorly in at least one KPI.

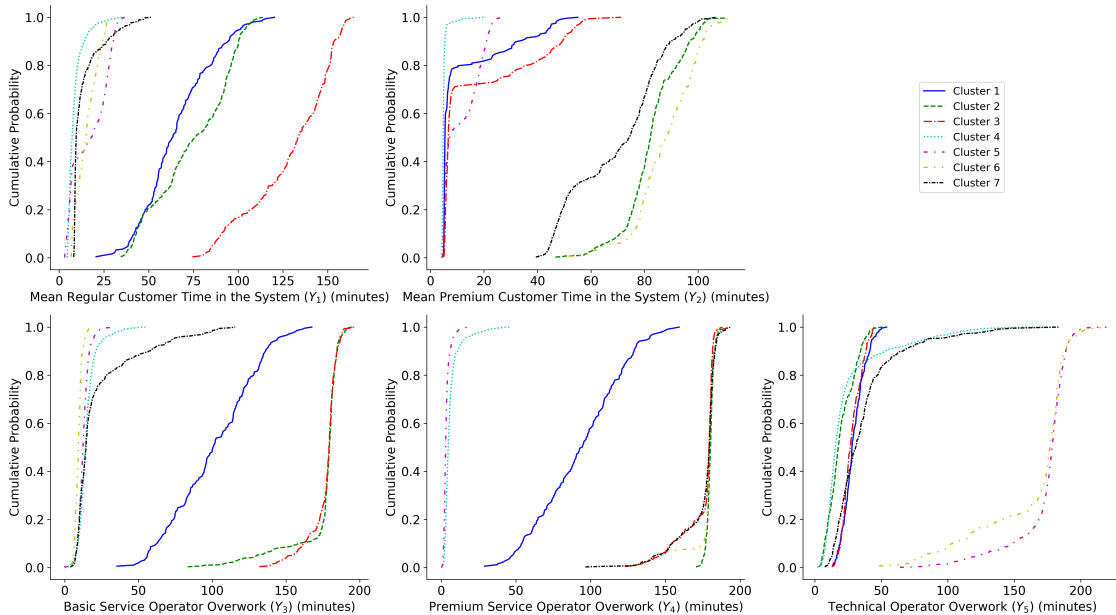


Figure 2: Marginal cdfs for each KPI for each barycenter, for a fixed number of operators.

Having identified a good cluster, we examine the correlation matrix of Cluster 4 in Figure 3. We observe a positive correlation between the overwork of premium service operators and the time spent by both types of customers in the call center, as well as the mean overwork of basic service operators. This suggests that for staffing configurations in Cluster 4, a high overwork time for premium service operators on any given day is associated with both regular and premium customers spending more time in the call center than usual and basic service

operators experiencing more overwork time than average. We compare to the correlation matrix of Cluster 5, which performs very well in the first four KPIs but poorly in terms of mean overwork for technical operators. In Figure 3, we observe a strong negative correlation between the mean time in the system of regular and premium customers.

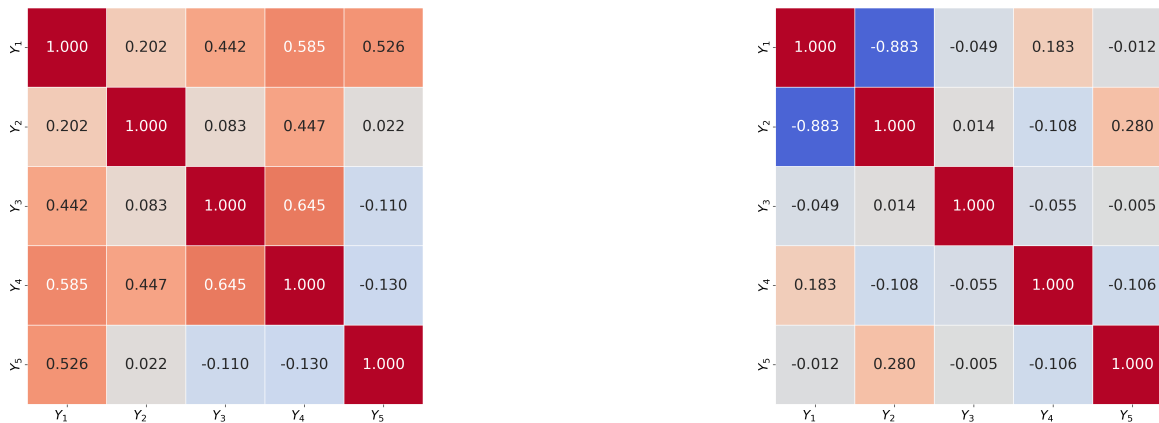


Figure 3: (Left) Correlation matrix for Cluster 4. (Right) Correlation matrix for Cluster 5.

As seen in Figure 4, the staffing configurations that make up Cluster 4 are characterized by having a moderate number of technical operators and a variable number of basic service and premium service operators, where the number of basic service operators is as low as 1 in some configurations. The decision maker might want to identify the staffing configuration among those in Cluster 4 that, say, minimizes the total staffing costs. For instance, if the staffing costs for basic service, premium service, and technical operators were 4, 1, and 1, respectively, then configuration (7, 28, 14) would be the cheapest.

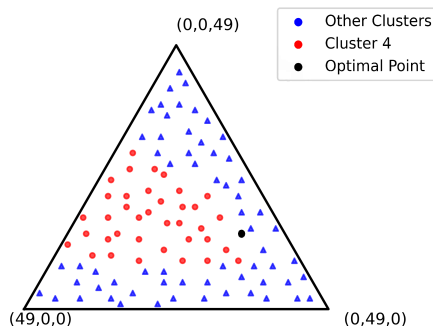


Figure 4: Simulated staffing configurations, represented as triplets of (# of premium service operators, # of basic service operators, # of technical operators). Configurations in Cluster 4, including the optimal staffing configuration (7, 28, 14), are highlighted.

4.2 Staffing Subject to a Budget

Staffing-cost considerations could alternatively be incorporated into the design of the experiment. As a follow-up to the staffing-cost analysis above, suppose the decision maker’s objective were to find a staffing configuration with a desirable output distribution among those having total costs between 50 and 55. There are 2,143 feasible staffing configurations and, as before, we uniformly select 100 configurations, simulate each for 40 days, and apply Algorithm 2 on the results. The silhouette index recommends five clusters; the marginal distributions of the corresponding barycenters are shown in Figure 5. Unlike in the previous experiment, no cluster dominates across all five KPIs: each cluster performs very well in at least one KPI, but suffers in other aspects. The decision maker’s priorities play a crucial role in balancing the tradeoffs across KPIs. For instance, if providing good customer service is more important than ensuring favorable conditions for operators, then Cluster 1 is preferable. Conversely, if keeping operators’ overwork low is a priority, then Cluster 3 might be preferred.

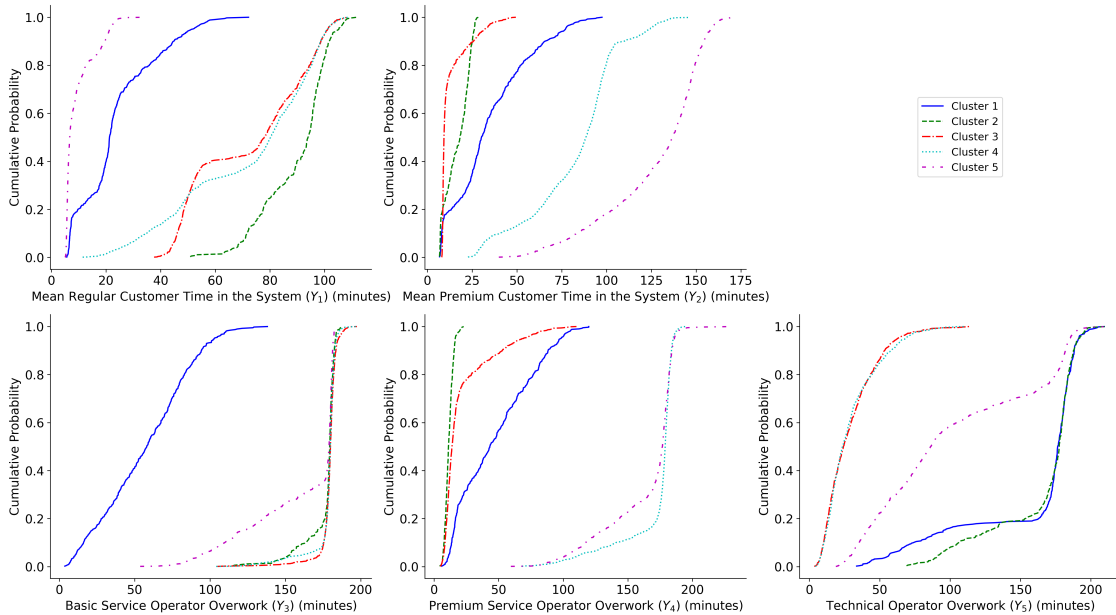


Figure 5: Marginal cdfs for each KPI for each barycenter, for staffing subject to a budget.

4.3 Monitoring Queue Lengths

In this experiment, we illustrate an approach that enables a decision maker to monitor the system in real time and use offline clustering to make staffing adjustments. In our setup, the system consists of 22 basic service, 9 premium service, and 8 technical operators, with other system specifications remaining the same as before. The state of the system is represented by a 4-dimensional vector consisting of the queue lengths for regular and premium customers for initial service, and the queue lengths for regular and premium customers for technical service. For a given state, we consider three KPIs: the mean utilization of all operators, the sum of the maximum waiting times of regular and premium customers in the technical queue, and the total number of customers who abandoned the queues (referred to as customer churn), all measured over a one-hour period when starting in that state. To construct a set of scenarios

for our offline experiment, we first simulate the system for 5000 days, recording the states at the beginning of each hour along with the corresponding output vector after an hour of observation. We restrict our attention to those states that were observed 10 or more times, of which there were 113. Algorithm 2 groups the output distributions into three clusters, the barycenters of which are depicted in Figure 6. Across all three performance metrics, Cluster 1 performs the best, Cluster 2 performs moderately well, and Cluster 3 performs the worst.

We now have the tools to monitor and classify the states visited during a new day by considering the state’s two nearest neighbors, as measured in terms of the queue lengths. When the current state’s two nearest neighbors belong to Cluster 1, we anticipate good performance in the next hour. Conversely, having both nearest neighbors in Cluster 2 suggests high customer churn and moderate operator utilization, with minimal impact on maximum waiting times. If both nearest neighbors belong to Cluster 3, poor performance across all metrics is expected in the next hour. There will be cases where the nearest neighbors are of different kinds, i.e., we find ourselves in a transition state between clusters. When this is the case, the decision maker should closely monitor trends and be prepared to take preventive actions, such as adjusting staffing in bottleneck areas or reallocating roles among cross-trained operators in a call-center context.

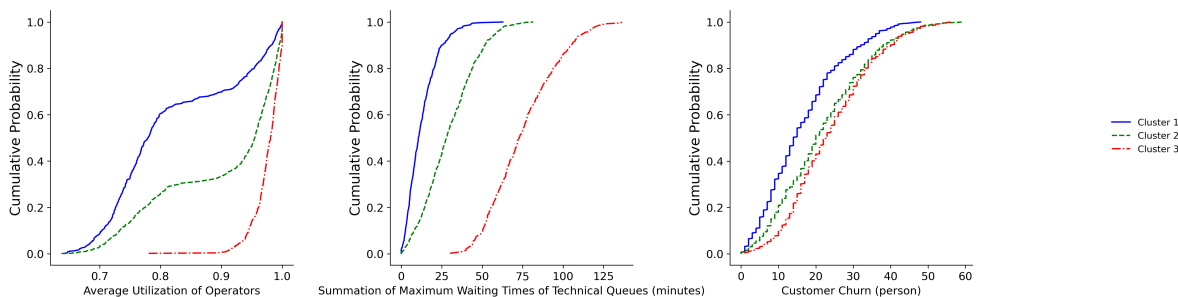


Figure 6: Marginal cdfs for each KPI for each barycenter, for state online monitoring.

Figure 7 illustrates this monitoring approach over the course of one day. The system starts the day with empty queues (a good state), but before long it begins to oscillate between good and moderate states, before settling into a moderate state around 8:30 and remaining there until 11:15 with occasional transitions. Around 12:30, the system briefly shifts to a bad state, before returning to a moderate state until about 13:30, after which all states are bad. The dashed area represents the times when the call center will be closed within the next hour, but the state classifications during this period can still be useful. The plot suggests several times where preventive action could be taken, e.g., around 11:20, when the system first enters an estimated bad state. A risk-averse decision maker might take preventive action at this time, but if they had waited to see if the situation persisted, they would have discovered that the system recovered on its own. Alternatively, the decision maker could intervene after observing bad states for some given duration. Each approach has its merits, catering to different risk tolerances and operational strategies.

5 Conclusion

This paper introduces an efficient agglomerative clustering algorithm for multivariate empirical distributions, motivated by the setting of analyzing simulation output data. Clus-

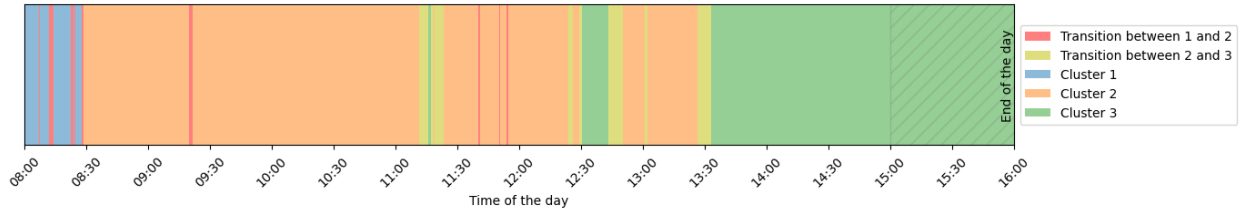


Figure 7: State monitoring of a new day with clustering and classification.

tering simulation output data by scenario can be a powerful approach for anomaly detection, pre-optimization, and classification in online monitoring. Future research directions include clustering simulation output distributions in a streaming-data setting and clustering simulation sample paths, which can provide deeper insights into dynamic system behavior.

References

- Abdallah, Imad, Tatsis, Konstantinos, & Chatzi, Eleni. 2020. Unsupervised local cluster-weighted bootstrap aggregating the output from multiple stochastic simulators. *Reliability Engineering & System Safety*, **199**, 106876.
- Altschuler, Jason, Niles-Weed, Jonathan, & Rigollet, Philippe. 2017. Near-linear time approximation algorithms for optimal transport via Sinkhorn iteration. *Advances in Neural Information Processing Systems*, **30**.
- Arjovsky, Martin, Chintala, Soumith, & Bottou, Léon. 2017. Wasserstein generative adversarial networks. *Pages 214–223 of: International Conference on Machine Learning*. PMLR.
- Benamou, Jean-David, Carlier, Guillaume, Cuturi, Marco, Nenna, Luca, & Peyré, Gabriel. 2015. Iterative Bregman projections for regularized transportation problems. *SIAM Journal on Scientific Computing*, **37**(2), A1111–A1138.
- Chakraborty, Saptarshi, Paul, Debolina, & Das, Swagatam. 2020. Hierarchical clustering with optimal transport. *Statistics & Probability Letters*, **163**, 108781.
- Cuturi, Marco. 2013. Sinkhorn distances: Lightspeed computation of optimal transport. *Advances in Neural Information Processing Systems*, **26**.
- Eisen, Michael B, Spellman, Paul T, Brown, Patrick O, & Botstein, David. 1998. Cluster analysis and display of genome-wide expression patterns. *Proceedings of the National Academy of Sciences*, **95**(25), 14863–14868.
- Henderson, Keith, Gallagher, Brian, & Eliassi-Rad, Tina. 2015. EP-MEANS: An efficient nonparametric clustering of empirical probability distributions. *Pages 893–900 of: Proceedings of the 30th Annual ACM Symposium on Applied Computing*.
- Horvath, Blanka, Issa, Zacharia, & Muguruza, Aitor. 2021. Clustering market regimes using the Wasserstein distance. *arXiv preprint arXiv:2110.11848*.
- Jain, Anil K. 2010. Data clustering: 50 years beyond K -means. *Pattern Recognition Letters*, **31**(8), 651–666.
- Jain, Anil K, Murty, M Narasimha, & Flynn, Patrick J. 1999. Data clustering: A review. *ACM Computing Surveys (CSUR)*, **31**(3), 264–323.
- Karthikeyan, B, George, Dipu Jo, Manikandan, G, & Thomas, Tony. 2020. A comparative study on k -means clustering and agglomerative hierarchical clustering. *International Journal of Emerging Trends in Engineering Research*, **8**(5), 1600–1604.
- Li, Haidong, Lam, Henry, & Peng, Yijie. 2024. Efficient learning for clustering and optimizing context-dependent designs. *Operations Research*, **72**(2), 617–638.
- Loureiro, Antonio, Torgo, Luis, & Soares, Carlos. 2004. Outlier detection using clustering methods: A data cleaning application. *In: Proceedings of KDNets Symposium on Knowledge-based Systems for the Public Sector*.

- Mur, Angel, Dormido, Raquel, Duro, Natividad, Dormido-Canto, Sebastian, & Vega, Jesús. 2016. Determination of the optimal number of clusters using a spectral clustering optimization. *Expert Systems with Applications*, **65**, 304–314.
- Murtagh, Fionn, & Contreras, Pedro. 2012. Algorithms for hierarchical clustering: An overview. *Wiley Interdisciplinary Reviews: Data Mining and Knowledge Discovery*, **2**(1), 86–97.
- Pappas, Thrasyvoulos N, & Jayant, Nikil S. 1989. An adaptive clustering algorithm for image segmentation. *Pages 1667–1670 of: International Conference on Acoustics, Speech, and Signal Processing*. IEEE.
- Peng, Yijie, Xu, Jie, Lee, Loo Hay, Hu, Jianqiang, & Chen, Chun-Hung. 2018. Efficient simulation sampling allocation using multifidelity models. *IEEE Transactions on Automatic Control*, **64**(8), 3156–3169.
- Peyré, Gabriel, & Cuturi, Marco. 2019. Computational optimal transport: With applications to data science. *Foundations and Trends® in Machine Learning*, **11**(5-6), 355–607.
- Riess, Lorenz, Beiglböck, Mathias, Temme, Johannes, Wolf, Andreas, & Backhoff, Julio. 2023. The geometry of financial institutions—Wasserstein clustering of financial data. *arXiv preprint arXiv:2305.03565*.
- Rubner, Yossi, Tomasi, Carlo, & Guibas, Leonidas J. 2000. The earth mover’s distance as a metric for image retrieval. *International Journal of Computer Vision*, **40**, 99–121.
- Santambrogio, Filippo, & Wang, Xu-Jia. 2016. Convexity of the support of the displacement interpolation: Counterexamples. *Applied Mathematics Letters*, **58**, 152–158.
- Shahapure, Ketan Rajshekhar, & Nicholas, Charles. 2020. Cluster quality analysis using silhouette score. *Pages 747–748 of: 2020 IEEE 7th International Conference on Data Science and Advanced Analytics (DSAA)*. IEEE.
- Villani, Cédric. 2009. *Optimal Transport: Old and New*. Vol. 338. Springer, Berlin, Germany.
- Wedel, Michel, & Kamakura, Wagner A. 2000. *Market Segmentation: Conceptual and Methodological Foundations*.
- Ye, Jianbo, Wu, Panruo, Wang, James Z, & Li, Jia. 2017. Fast discrete distribution clustering using Wasserstein barycenter with sparse support. *IEEE Transactions on Signal Processing*, **65**(9), 2317–2332.
- Zhang, Zishi, & Peng, Yijie. 2024. Sample-Efficient Clustering and Conquer Procedures for Parallel Large-Scale Ranking and Selection. *arXiv preprint arXiv:2402.02196*.
- Zhuang, Yubo, Chen, Xiaohui, & Yang, Yun. 2022. Wasserstein K -means for clustering probability distributions. *Advances in Neural Information Processing Systems*, **35**, 11382–11395.